

TABLE II. Parameters for an exponentially screened Coulomb potential in silicon.

	Screening constant b (\AA^{-1})	Charge product $Z_1 Z_2$	Proton charge $Z_1 Z_2 / 14$
Experimental,			
$l_{111} = 1.1757 \text{ \AA}$	1.51 ± 0.85	13.4 ± 5.3	0.96 ± 0.38
$l_{111} = 1.5675 \text{ \AA}$	1.68 ± 0.30	14.1 ± 3.6	1.01 ± 0.26
$l_{111} = 1.1757,$ 1.9594 \AA	2.24 ± 0.55	18.2 ± 5.6	1.30 ± 0.40
Thomas-Fermi theory	1.543	14	1

bilities. In Table II, the potential parameters deduced from the data using Eq. (2) are shown. The two choices of $\{111\}$ spacing make little difference in the results, the greater spacing in the second case being largely offset by the greater density

of atoms in the effective defining planes. A larger effect is produced if the $\{111\}$ channel is defined using both sets of bounding planes, located at their correct positions. In this case the exponential in Eq. (2) is replaced by the sum of two, each with its own value of l . In all cases, the calculated proton charge is in satisfactory agreement with the expected value. The screening constant is also reasonably close to that expected theoretically if the electron density in silicon is given by the Thomas-Fermi model⁸ and the Molière approximation is used for the screening function. This agreement, which is similar to that achieved for gold,⁴ lends considerable confidence to the underlying model.

The authors are grateful to Bryant Welch for assistance with sample preparation and with taking the experimental data, and to D. K. Holmes and W. E. Atkinson for several helpful discussions of the theory of these experiments.

*Research sponsored in part by the U. S. Atomic Energy Commission under contract with Union Carbide Corporation.

¹H. O. Lutz, S. Datz, C. D. Moak, and T. S. Noggle, *Phys. Rev. Letters* **17**, 285 (1966); S. Datz, C. D. Moak, T. S. Noggle, B. R. Appleton, and H. O. Lutz, *Phys. Rev.* **179**, 315 (1969); S. Datz, C. D. Moak, B. R. Appleton, M. T. Robinson, and O. S. Oen, in *Atomic Collision Phenomena in Solids*, edited by D. W. Plamer, M. W. Thompson, and P. D. Townsend (North-Holland, Amsterdam, 1970), p. 374.

²M. T. Robinson, *Phys. Rev.* **179**, 327 (1969).

³M. T. Robinson, following paper, *Phys. Rev. B* **4**, 1461 (1971).

⁴B. R. Appleton, S. Datz, C. D. Moak, and M. T. Robinson, preceding paper, *Phys. Rev. B* **4**, 1452 (1971).

⁵F. H. Eisen, *Can. J. Phys.* **46**, 561 (1968).

⁶F. H. Eisen (unpublished).

⁷G. Molière, *Z. Naturforsch.* **2a**, 133 (1947).

⁸P. Gombas, in *Handbuch der Physik*, edited by S. Flügge (Springer, Berlin, 1956), Vol. 36, p. 109.

Deduction of Interaction Potentials from Planar-Channeling Experiments*

Mark T. Robinson

Solid State Division, Oak Ridge National Laboratory, Oak Ridge, Tennessee 37830

(Received 2 November 1970)

A model is presented which allows planar-channeling data to be used to deduce the parameters of the interaction potential between the channeled ions and the atoms of the solid and which relates the stopping power of channeled ions to that of randomly directed ones. The analysis is based on the experimental observation of the proportionality between the stopping power and the transverse oscillation frequency of ions traversing the planar channels of thin crystal targets. It is applied to data on He, O, and I ions transmitted through the $\{111\}$ and $\{100\}$ channels of Au crystals and on H ions transmitted through the $\{111\}$ and $\{110\}$ channels of Si crystals. For both targets, the screening constants of the interaction potentials are in excellent agreement with recent Hartree calculations. The same potentials allow the calculation of random stopping powers from the channeling data which are in good agreement with observation, especially when account is taken of thermal vibrations of the lattice atoms.

INTRODUCTION

In an earlier paper,¹ a model was described for the interpretation of the energy-loss spectra observed²⁻⁶ in beams of energetic ions transmitted through planar channels in thin single-crystal tar-

gets. The ions were regarded as executing transverse anharmonic oscillations under the influence of the planes of lattice atoms bordering the channel and as losing energy at a rate which depended upon their position within the channel. After choosing a particular plausible form for the interaction

potential between the ions and the lattice atoms, it was possible to find empirically a correspondingly simple function to represent the coordinate dependence of the stopping power and to make a quantitative comparison of the model with experimental data⁴ on the energy-loss spectra of 3-MeV ⁴He ions and 60-MeV ¹²⁷I ions transmitted through the {111} and {100} channels of thin gold crystals. The essential feature of the data which made this comparison possible was the observation that the stopping power of these ions was accurately proportional to the frequency of their transverse oscillations in the channels. This proportionality has now been observed also for 15- and 21.6-MeV ¹²⁷I ions^{5,6} and for 10-MeV ¹⁶O ions⁶ transmitted through the {111} and {100} channels of gold targets and for 0.4-MeV H ions⁷ transmitted through the {111} and {110} channels of silicon targets. It seems reasonable, therefore, to adopt this relationship between the stopping power and the oscillation frequency of channeled ions as an empirical first principle and to examine its consequences for the interpretation of the experimental energy-loss spectra. Using this procedure, it is possible to represent the interaction potential between the ions and the target atoms by almost any desired function and to deduce the form of the corresponding stopping-power function. The analysis also leads to a quantitative connection between the channeling data and the ordinary stopping power of randomly directed ions. Experimental data may be used to evaluate the parameters of the interaction potential and of its conjugate stopping-power function. When the latter is used to compute the random stopping power, a particularly sensitive test of the model results.

DESCRIPTION OF MODEL

Because of their high velocities and relatively large impact parameters, channeled ions suffer only very small deflections in their encounters with individual lattice atoms. The correlated nature of successive collisions slowly turns the ions away from a plane of atoms and directs them back across the channel, as long as their direction of motion makes a small enough angle with the plane. In this circumstance, and when incidence parallel to principal crystallographic axes is avoided, the atomic nature and regular structure of the planes bordering the channel may be ignored and the ions may be represented as interacting with the planar continuum potential

$$V_1(\bar{x}) = 4\pi\kappa\rho l \int_{\bar{x}}^{\infty} rV(r)dr, \quad (1)$$

where $V(r)$ is the interaction potential between an ion and a lattice atom separated by a distance r , ρ is the atomic density of the target, l is the half-

width of the planar channel, \bar{x} is the length of the normal from the ion to the plane of lattice atoms, and κ is a factor allowing for the possibility that there may be parallel channels of different widths in some crystal structures (or, put alternatively, that the atomic density in a plane differs from $2\rho l$).⁷ The channeled ions move between a pair of planes, that is, they oscillate in the planar-channel potential

$$V_2(x) = V_1(l+x) + V_1(l-x), \quad -l \leq x \leq l \quad (2)$$

where the origin is taken halfway between the two planes, a distance l from each. The coordinates used in the dynamical problem are shown in Fig. 1. Since the angle between the direction of motion of the ions and the bordering atomic planes is small ($< \sim 0.5$ deg), $\sin \psi = \tan \psi = \psi$ and $\cos \psi = 1$ are sufficiently accurate approximations. It is then possible to identify the velocity of the ion $(2E/m)^{1/2}$, where m is the mass of the ion and E is its kinetic energy, with its longitudinal component, and to regard the stopping power as influencing this component only. The transverse motion may then be considered to continue without damping. In this approximation, an ion oscillates with a "frequency" ω defined by

$$\omega^{-1} = 2 \int_0^{x_m} [V_2(x_m) - V_2(x)]^{-1/2} dx, \quad 0 \leq x_m \leq l \quad (3)$$

where x_m is the amplitude of the oscillation. Note that ω is not a true frequency: A factor $(2m)^{1/2}$ has been suppressed in Eq. (3) and in the experimental definitions of ω as well.^{1,6}

Empirically, it is found^{1,4-7} that the stopping power of an ion, averaged over its oscillatory motion but corrected to its incident energy, is proportional to its oscillation frequency:

$$\left(\frac{-dE}{dz} \right)_{E=E_0} = \alpha + \beta\omega, \quad (4)$$

where α and β are empirical constants. It will be assumed that the model stopping power is given by

$$S(x, E) = s_0 + s_1[\sigma(x) - 1], \quad (5)$$

where s_0 and s_1 depend on the ion energy. The spatial dependence of the stopping power is described by the function $\sigma(x)$, so normalized that $\sigma(0) = 1$. The object of the following analysis is to relate $\sigma(x)$ to the potential function $V_2(x)$. The parameter s_0 is the minimum stopping power observed for the channeled ions and is available from experimental data separately from α and β . When Eq. (5) is averaged over the oscillatory motion of the ion and the result is compared with Eq. (4), it is found that as long as the number of half-oscillations executed by the ion is integral, the experiments measure

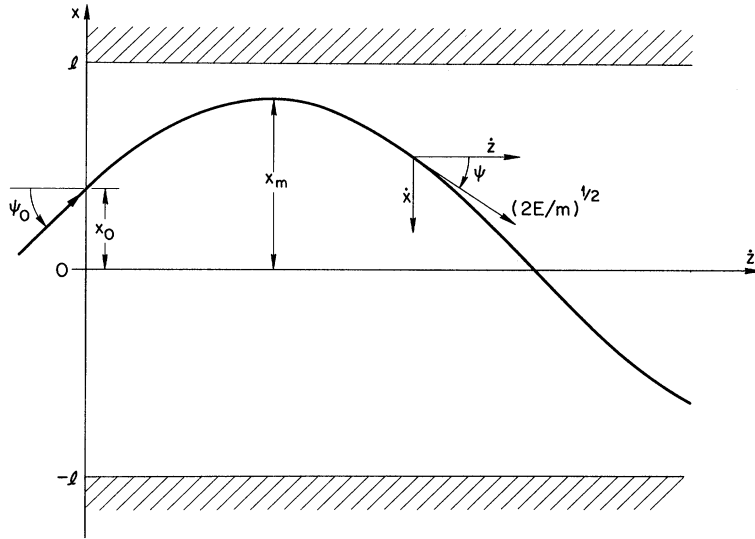


FIG. 1. Coordinates used to describe the planar-channeling model.

$$\alpha = s_0 - s_1, \quad (6)$$

$$\beta = 2s_1 \int_0^{x_m} \sigma(x) [V_2(x_m) - V_2(x)]^{-1/2} dx, \quad 0 \leq x_m \leq l. \quad (7)$$

These results apply in principle when the number of quarter-oscillations is integral, but each of these quarter-oscillations must be complete, that is, include both a node and an antinode. An experiment involving an odd number of quarter-waves has been described⁷ where the first one traversed is not complete, but is centered either on a node or on an antinode. In this instance, as in more general cases also, Eq. (7) is only approximate and errors may be introduced by its use.

In the previous work,¹ a particular form was assumed for $V_2(x)$ and an essentially empirical search located a function $\sigma(x)$ for which β , as given by Eq. (7), was constant. A more direct procedure is available, however. Equation (7) is an integral equation of the Abel type and is very easily solved.⁸ Assuming β to be constant, the result is

$$\sigma(x) = \frac{\beta}{\pi s_1} \frac{d}{dx} [V_2(x) - V_2(0)]^{1/2}, \quad 0 \leq x \leq l. \quad (8)$$

The correctness of this result may be verified by substituting it into Eq. (7) and performing the indicated integration. Since $V_2(x)$ is an even function, it is easily found that

$$\sigma(0) = \frac{\beta}{2^{1/2} \pi s_1} [V_2''(0)]^{1/2}, \quad (9)$$

where the primes represent differentiation with respect to x . As long as $V_2''(0)$ does not vanish, the normalization $\sigma(0) = 1$ may be imposed, with the result that

$$\sigma(x) = \frac{d}{dx} \left(\frac{2}{V_2''(0)} [V_2(x) - V_2(0)]^{1/2} \right), \quad 0 \leq x \leq l. \quad (10)$$

The function $\sigma(x)$ is a measure, not only of the stopping power of the ions, but also of the anharmonicity of the planar-channel potential: It deviates from unity only insofar as $V_2(x)$ deviates from harmonicity. If the potential function assumed previously,¹ namely,

$$V_2(x) = V_0 \cosh bx, \quad (11)$$

is inserted into Eq. (10), it is immediately found that the conjugate stopping-power function is

$$\sigma(x) = \cosh \frac{1}{2} bx, \quad (12)$$

in agreement with the earlier result, which, in spite of its empirical origin, is now seen to be uniquely related to the potential (11). The analysis, however, is no longer restricted to this potential function. The experimental energy-loss spectra^{6,7} are conveniently presented in terms of the curvature parameter:

$$y \equiv 2\pi^2 (s_0 - \alpha)^2 / \beta^2 l \quad (13a)$$

$$= V_2''(0) / l \quad (13b)$$

$$= 2V_1''(l) / l = -8\pi\rho\kappa [V(l) + lV'(l)], \quad (13c)$$

where the second line employs Eqs. (6) and (9) and the third requires Eqs. (1) and (2). Thus, from the experimental data on the stopping power of ions as a function of their oscillation frequencies, the curvature of the planar-channel potential at the center of the channel, or its equivalents as given by Eq. (13), may be determined directly. Given data for a sufficient number of different channels with distinct values of l , the parameters of any potential function may be evaluated. Examples of this procedure have

been given elsewhere^{1,6,7} and will be discussed in more detail below. It must be emphasized that no assumptions have been made in the above analysis about the nature of the functions $V_2(x)$ and $\sigma(x)$, apart from their evenness and mathematical properties necessary to ensure convergence of the integral in Eq. (7). The experimental curvature parameters are independent of assumptions about the potential.

The solution of the integral equation (7) can also be carried out for the case where β is not constant but depends on ω . This general solution cannot be used to analyze the experimental data, however, since to do so it is necessary to know the amplitude corresponding to each frequency. If this were known, the potential function could be determined directly from experimental data without reference to the present procedure, an objective² which is frustrated by the apparently unattainable precision required in angular measurements. It is easily seen from Fig. 1 that for particles on a particular trajectory, labeled by its energy loss,^{1,2,4} we have

$$x_m = \int_{z_1}^{z_2} \psi(z) dz, \quad (14)$$

where the limits on the integral correspond to those pathlengths for which the ion emerges from the crystal with $\psi = 0$ and ψ a maximum, respectively. Then, if the uncertainty in measuring an angle is $\delta\psi$, the corresponding error in estimating the oscillation amplitude is

$$\delta x_m = (z_2 - z_1)\delta\psi = \lambda\delta\psi/4 = (E_0^{1/2}/2\omega)\delta\psi, \quad (15)$$

where the second and third forms follow from the definition of the oscillation wavelength λ and its relation to the oscillation frequency.^{1,4-7} Since $\lambda \sim 10^3 \text{ \AA}$, to achieve an amplitude accuracy of $\sim 10^{-2} \text{ \AA}$ —about 1% of a channel half-width—requires the determination of angles with a precision ~ 10 sec, very unlikely to be attainable considering the divergence of the incident beam, the acceptance angle of the detector, and the considerable mosaic spread in the crystals. It is indeed fortunate that the alternative procedure represented by the preceding analysis is available.

Since the curvature parameters do not determine a potential function uniquely, but only the connection between the potential and its conjugate stopping function, it is necessary to seek an independent method of testing any particular choice of potential function. The stopping power of ions moving randomly through the target may be measured easily. The motion of such ions is not much influenced by the correlated scatterings which characterize channeling: As they cross a channel, their velocities are nearly unaltered. Thus, for an ion moving randomly through the crystal, the model stopping power, Eq. (5), may be averaged to yield the random stopping power

$$-\left(\frac{dE}{dz}\right)_{\text{random}} \equiv \hat{S} = s_0 - s_1 + \frac{s_1}{l} \int_0^l \sigma(x) dx \quad (16)$$

or, using Eqs. (6) and (8),

$$\hat{S} = \alpha + (\beta/\pi l)[V_2(l) - V_2(0)]^{1/2}. \quad (17)$$

For any assumed two-parameter potential, experimental channeling data may be used with Eq. (13) to evaluate the parameters and the values obtained may be used in Eq. (17) to calculate the random stopping power. The result may be compared with experimental observation and should, moreover, be independent of the channel orientation. It is interesting to note that the so-called critical channeling angle,⁹ that is, the angle with respect to the planar channel at which the ion can break through the continuum potential, is given by

$$\psi_c = E^{-1/2}[V_2(l) - V_2(0)]^{1/2}. \quad (18)$$

An interesting test of the planar-channeling model could be made by using Eqs. (17) and (18) to relate the random stopping power to the critical angle. Unfortunately, critical angles are difficult to measure accurately, largely because of the mosaic spread in the target orientation, so that the comparison cannot be made very precisely.

The procedure for deducing interaction potentials from planar-channeling data may now be summarized. Curvature parameters, determined experimentally for as many different channels as possible, provide the necessary data. If enough data were available, they could be used for the numerical integration of the differential Equation (13c). For more limited data, the parameters of an assumed potential function can be evaluated from Eq. (13b). In either case, a check on the results can be made by calculating the random stopping power through Eq. (17). The latter method will be used to study several interaction potentials which have been widely used for descriptions of atomic collisions in solids, using the data available for planar channeling in gold⁶ and silicon.⁷

APPLICATION TO PLANAR CHANNELING IN GOLD

The potentials to be considered in the gold crystals are defined in Table I, which also gives the values of the ion-independent parameter in each case, that is, the parameter determined by the ratio y_{111}/y_{100} . Uncertainties in the parameters are about $\pm 10\%$.

Since inverse-power potentials are frequently used in treating atomic scattering,¹⁰ it is of interest to note that the gold planar-channeling data indicate an interaction varying as $r^{-7/2}$ near the centers of the two channels. This interaction cannot extend all the way to the atomic planes, however, as it

TABLE I. Definitions and ion-independent parameters of some interatomic potential functions, based on experimental curvature parameters (Ref. 6) for several ions in gold.

Potential	Definition of $V(r)$	Ion-independent parameter ^a
Power	a_k/r^k	$k=3.50$
Born-Mayer (BM)	$C_{BM}e^{-r}/a_{BM}$	$a_{BM}=0.230 \text{ \AA}$
Screened Coulomb	$(Z_1Z_2e^2/r)\phi(r)$	
Power (PS)	$\phi(r) = 1 - r[r^m + c^m]^{-1/m}$	$m > 2.50$
Thomas-Fermi (TF)	$\phi(r) = \phi_{TF}(r/a_{TF})$	$a_{TF}=0.0172 \text{ \AA}$
Bohr (B)	$\phi(r) = C_B e^{-br}$	$b = 3.22 \text{ \AA}^{-1}$ $1/b = 0.310 \text{ \AA}$
Exponential sum	$\phi(r) = \sum_{i=1}^3 \alpha_i e^{-\beta_i r}$	
Molière (M)	$\left\{ \begin{array}{l} [\alpha] = [0.35, 0.55, 0.10] \\ [\beta] = [b, 4b, 20b] \end{array} \right.$	
Hartree (H) ^b	$\left\{ \begin{array}{l} [\alpha] = [0.25, 0.50, 0.25] \\ [\beta] = [b, 2.43b, 8.77b] \end{array} \right.$	

^aBased on the experimental value (Ref. 6) $y_{111}/y_{100} = 0.604$; $l_{111} = 1.1774 \text{ \AA}$; $l_{100} = 1.0197 \text{ \AA}$.

^bThe parameter values given apply only to Au.

leads to an infinite random stopping power. Closely related to the inverse-power potentials are a family of screened Coulomb potentials with power-screening functions, PS in Table I. This potential with the value $m=2$ was used by Lindhard in his discussion of the theory of axial channeling.⁹ More recently, it has been employed by Machlin *et al.*¹¹ in an analysis of some experimental energy-loss data for 0.1-MeV protons in gold {100} channels. The present data, however, preclude the use of $m \leq \frac{5}{2}$, since for these cases $c^m \leq 0$ results. Since it has three parameters, the PS potential could be caused to fit the curvature parameters for the two channels and the random stopping power as well, by selecting appropriate values of m , c , and Z_1Z_2 . The theoretical significance of this potential is dubious enough, however, for this not to have been attempted. Since the planar-channeling results are clearly inconsistent with the value $m=2$, the agreement which Machlin *et al.*¹¹ find between their calculations and their experiment must be fortuitous.

The screening length obtained from the planar-channeling data for a Born-Mayer (exponential) potential is in good agreement with the value 0.201 Å deduced by Thompson¹² for the interaction of gold atoms using observations of the bulk modulus and the (110) focusing energy. It is somewhat smaller than the value 0.287 Å suggested by Abrahamson¹³ for the same atoms. This implies that over the range $r > 1 \text{ \AA}$, the shape of the interaction potential between a gold atom and other particles is not very sensitive to the nature of the partner. The Born-Mayer form is not especially suitable for close encounters, however, since it does not possess the requisite Coulomb core. This failing is especially

evident when the random stopping power is evaluated (cf. Table III and the subsequent discussion). Because of this failure, the empirical values of C_{BM} are not tabulated.

The remaining potentials in Table I are all of the screened Coulomb type. For them, besides a screening constant, the data have been used to evaluate the apparent ionic charges $q_1 = Z_1Z_2/79$. The viewpoint is that since the screening constant is independent of the ion and its energy,⁶ it describes the distribution of the screening electrons in the gold crystal. The three ions are then "test charges" which sample the electron density in the crystal. One test of a potential then becomes the plausibility of the deduced ionic charge. The values obtained are compared in Table II with the equilibrium charge states observed in the transmitted beam. In the case where the Thomas-Fermi screening function¹⁴ is used, the theoretically expected screening length is 0.109 Å, more than six times larger than the observed value. At the same time, the apparent ionic charges are very large, so much so, in fact, as to be absurd. The small screening length and the large ionic charges all result from the well-known fact that the Thomas-Fermi (TF) screening function varies too slowly with distance at large

TABLE II. Ionic charges deduced for several ions in gold using experimental curvature parameters (Ref. 6).

Ion	Energy (MeV)	Potential	Ionic charge $q_1 = Z_1Z_2/79$	Equilibrium ionic charge
He	3	TF	61	2
		M	1.5	
		H	2.1	
		HV ^a	2.0	
O	10	TF	146	5.5 ^b
		M	3.6	
		H	5.0	
		HV	4.8	
I	15	TF	398	13 ^c
		M	19	
		H	27	
		HV	26	
	21.6	TF	892	15 ^c
		M	22	
		H	31	
		HV	30	
60	60	TF	1200	22 ^c
		M	29	
		H	41	
		HV	40	

^aHV indicates the Hartree (H) potential of Table I, corrected for the effects of thermal vibrations.

^bF. W. Martin, B. R. Appleton, L. B. Bridwell, M. D. Brown, S. Datz, and C. D. Moak (unpublished).

^cC. D. Moak, H. O. Lutz, L. B. Bridwell, L. C. Northcliffe, and S. Datz, Phys. Rev. 176, 427 (1968).

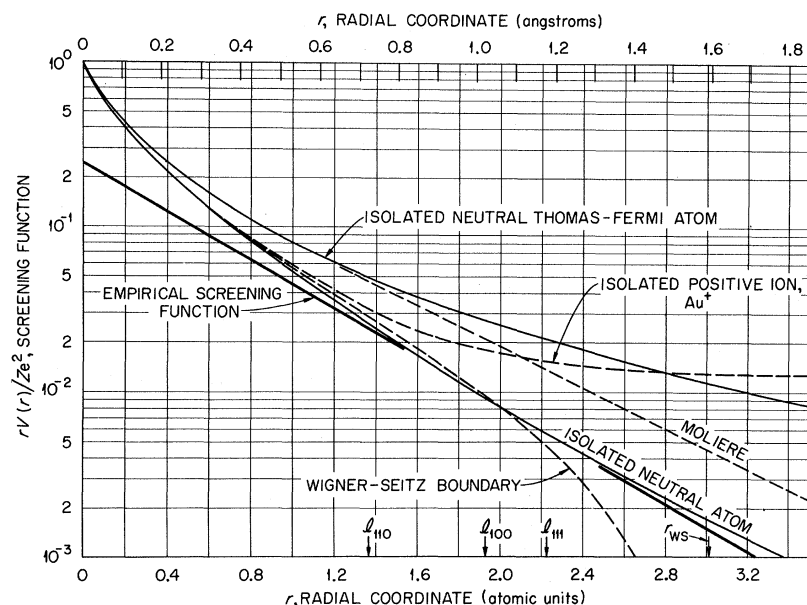


FIG. 2. Comparison of the empirical potential deduced from planar-channeling data in Au with Thomas-Fermi and Hartree potentials describing the electron distributions in the isolated Au atom, the isolated Au⁺ ion, and the Au atom confined to a spherical Wigner-Seitz cell (radius r_{ws}).

distances from the nucleus. The procedure for fitting the potential to the data tries to compensate for this by producing the parameters tabulated. No attempt has been made to evaluate the random stopping power for the TF potential.

The three potentials remaining in Table I have screening functions which reduce to a single exponential in the range of distances near the centers of the two gold channels. Consequently, they all yield the same value of the screening constant. The Molière potential¹⁵ was proposed as an approximation to the Thomas-Fermi screening function, but has the advantage of falling off much more rapidly with distance. The observed screening constant is nearly one-fifth larger than the theoretically expected value 2.75 \AA^{-1} . It is, however, in excellent agreement with the value expected from a machine calculation discussed by Tucker *et al.*¹⁶ They describe a relativistic self-consistent-field program for the evaluation of atomic wave functions. The electrostatic potential of an isolated gold atom in its ground state, as produced by this program, is designated as the Hartree potential in Table I. It is compared in Fig. 2 with some related potentials calculated by the same program, as well as with the Thomas-Fermi and Molière functions, and with the empirically deduced potential. The last is simply an exponential screening function with the empirical value of b , passed through the Hartree potential midway between the centers of the two channels. It is clear from the figure that confining the Au atom to a spherical Wigner-Seitz cell to simulate solid-state effects does not make an important alteration in the potential and that the ion Au⁺ is not relevant to the present discussion. Like the Molière potential, the Hartree potential for gold

may be represented rather accurately by a sum of three exponentials, with the parameters listed in Table I. The influence of the thermal motion of the lattice atoms must also be considered. It is assumed that the displacements of the atoms normal to the channel plane are uncorrelated and are distributed according to a Gaussian. The effect of these displacements on exponentially screened Coulomb potentials has been described before.^{1,17,18} The Hartree potential of Table I, with allowance made for thermal vibrations, will be designated HV. The inclusion of thermal effects does not alter the empirically deduced screening constant but does influence slightly the value deduced for the apparent ionic charge. The apparent ionic charges deduced using the M , H , and HV potentials are listed in Table II. All three yield values for the two lighter ions in good agreement with observed equilibrium charge states. In the case of I ions, however, the calculated charges are, respectively, approximately 1.4, 2.0, and 1.9 times larger than the observed values. This suggests the approximate nature of the original view that the ions are merely test charges. Evidently the screening of the I nucleus by its own electrons varies significantly as the ion oscillates in the channel.

In Table III are displayed the values calculated for the random stopping power using some of the potentials from Table I. The Bohr-potential values assumed that $C_B = 0.35$; that is, one term only of the Molière potential was used. This corresponds to the potential used in earlier work.¹ The recent x-ray value of Synacek *et al.*¹⁹ was used for the mean-square vibrational amplitude of gold atoms. The result obtained for the random stopping power is rather insensitive to the choice of the vibration amplitude,

TABLE III. Random stopping powers computed using various interatomic potential functions and experimental curvature parameters (Ref. 6) for several ions in gold.

Ion	Energy (MeV)	Potential	Random stopping power (MeV/ μm)		Observed
			{111}	{100}	
He	3	BM	0.310	0.326	0.58 ^a
		B	0.489	0.510	0.54 ^b
		M	0.604	0.628	
		H	0.730	0.759	
		HV ^c	0.583	0.600	
O	10	BM	2.65	2.78	4.74 ^b
		B	3.53	3.59	
		M	4.10	4.11	
		H	4.73	4.70	
		HV ^c	3.94	3.98	
I	15	BM	3.71		9.0 ^d
		B	4.94		8.3 ^b
		M	5.73		
		H	6.58		
		HV ^c	5.49		
	21.6	BM	5.00	5.24	11.5 ^d
		B	6.77	7.04	10.9 ^b
		M	7.91	8.20	
		H	9.16	9.45	
		HV ^c	7.74	7.85	
	60	BM	13.4	13.2	23.9 ^d
		B	18.0	17.8	23.1 ^b
		M	21.0	20.8	
HV ^c		19.9	20.0		

^aG. W. Gobeli, Phys. Rev. **103**, 275 (1956); cf. W. Whaling, in *Handbuch der Physik*, edited by S. Flügge (Springer, Berlin, 1958), Vol. 34, p. 204.

^bL. C. Northcliffe and R. F. Schilling, Nucl. Data **A7**, 233 (1970).

^crms thermal-vibration amplitude 0.0792 Å (Ref. 19).

^dC. D. Moak and M. D. Brown, Phys. Rev. **149**, 244 (1966).

however, a 10% increase in the rms amplitude producing only about a 1% decrease in \hat{S} . All potentials used in Table III produce values of the random stopping power from {111} channeling data that are in very good agreement with the values from {100} data. This verifies one of the required features of the model. Furthermore, there is general agreement of the calculated values with observations. The Born-Mayer-potential results are always low, averaging about half of the observed values, this being due to the absence of the Coulomb core from the potential. The Bohr-potential calculations are somewhat better, but still do not account adequately for the observations. The Molière potential and the thermally corrected Hartree potential give results in close agreement with each other; the agreement with experiment is good for α particles, fair

for O ions, and poor to fair for I ions, depending on the energy. But this is just what is to be expected. The α particle is a bare nucleus with no accompanying electrons so that its effective charge is the same wherever it is in the channel. The other ions, however, carry a number of electrons. Hence, even though they may act essentially as test charges when near the center of a channel, as they approach closely to a lattice atom, screening of their nuclear charge by their own electrons must decrease and the interaction between the ions and the gold atoms must increase more rapidly than described by any of the potentials used here. This would lead in turn to higher random stopping powers than are listed in Table III. Nevertheless, the results obtained give encouraging support to the validity of the model which has been used.

A final test of the reasonableness of the potential derived from planar-channeling data is to evaluate the scale of oscillation amplitudes. This is done by using Eq. (13) to connect the amplitudes with the oscillation frequencies. In the upper part of Table IV, the minimum and maximum amplitudes deduced for each ion and channel using the Hartree potential are listed. Thermal-vibration effects were not included; they are not important even at the largest amplitude in the table. The extreme values of the amplitudes correspond to the extreme values of the observed oscillation frequencies and are, perhaps, somewhat subjective. Nevertheless, with one obvious exception, there is good agreement amongst the minimum amplitudes. There is similar agreement in the maximum amplitudes for the individual channels. Furthermore, these maximum amplitudes correspond in each case to the same distance of approach to the plane, an amount just less than 3 times the rms thermal-vibration amplitude. The unobserved particles of larger amplitude have been diverted by hard collisions into the so-called unaligned beam¹⁰ and will show the random energy loss.

TABLE IV. Oscillation amplitudes derived from planar-channeling data using the Hartree potential.

Ion	Energy (MeV)	Calculated oscillation amplitudes (Å)			
		{111}		{100}	
		min	max	min	max
He	3	0.431	0.874	0.434	0.765
O	10	0.455	0.977	0.437	0.867
I	15	0.420	1.011
	21.6	0.458	0.918	0.425	0.827
	60	0.407	0.920	0.216	0.756
Mean amplitudes $\langle x_m \rangle$		0.434	0.940	0.378	0.803
		± 0.020	± 0.048	± 0.094	± 0.046
Half-width l		1.1774		1.0197	
$l - \langle x_m \rangle_{\text{max}}$		0.237		0.217	
		± 0.048		± 0.046	

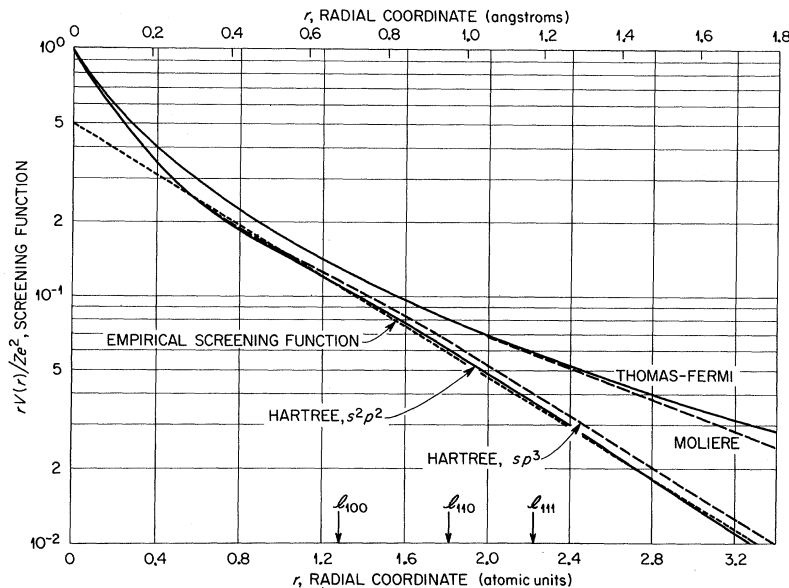


FIG. 3. Comparison of the empirical potential deduced from planar-channeling data in silicon with Thomas-Fermi and Hartree potentials describing the electron distributions in the isolated Si atom.

APPLICATION TO PLANAR CHANNELING IN SILICON

The application of the model to data on planar channeling in silicon⁷ presents certain difficulties, principally associated with the structure of the {111} channel. This channel is bordered by pairs of rather closely spaced planes, instead of by the single planes found in gold or in some other channels in silicon. In this case, it is necessary to replace Eq. (2) by

$$V_4(x) = V_1(l+x) + V_1(l-x) + V_1\left(\frac{2}{3}l+x\right) + V_1\left(\frac{2}{3}l-x\right), \quad (19)$$

where l is half the distance between the inner pair of planes (1.1757 Å in Si) and where κ in Eq. (1) is to be taken as $\frac{2}{3}$. The inclusion of both sets of bounding planes in treating the data on 0.4-MeV protons in Si is necessary, as is shown by the effects on the apparent screening constant of simpler descriptions of the {111} channel.⁷ The analysis of these data, paralleling the analysis of the gold data in every way, is summarized in Table V. The Hartree potential was calculated using the machine program described for gold¹⁶ for two different electronic configurations: s^2p^2 , the ground state of the isolated ion, and sp^3 , the ground state in the crystals. These two functions are compared in Fig. 3 with the empirically deduced potential as well as with the Thomas-Fermi and Molière functions. The s^2p^2 Hartree potential may be represented with moderate accuracy by the sum of two exponentials; the parameters are listed in Table V. The apparent proton charge given by the Hartree potential agrees well with the expected value. Again the random stopping powers calculated for the two orientations

are in good agreement with each other. In calculating \hat{S} from the {111} data, it was assumed that α and β were the same in the narrower channel as the experimental values in the wider channel. The agreement of the {110} and {111} values calculated for \hat{S} supports this assumption. The thermal-vibration amplitude of Si was taken from the x-ray studies of Batterman and Chipman.²⁰ Although the Hartree

TABLE V. Application of the model to 0.4-MeV protons in silicon {111} and {110} channels.

i Parameters of the Hartree potential for s^2p^2 Si:		
	$[\alpha] = [0.50, 0.50]$	$[\beta] = [b, 5b]$
ii Empirical potential parameters, $b = 2.24 \text{ \AA}^{-1}$:		
Potential	Proton charge q_1	
M	1.30	
H	0.91	
HV^a	0.90	
iii Calculated random stopping power (MeV/ μm):		
Potential	{111}	{110}
M	...	0.152
H	0.112	0.120
HV^a	0.0855	0.0832
	Observed ^b : 0.0675	
iv Calculated oscillation amplitudes (Å), Hartree potential:		
	{111}	{110}
min	0.493	0.206
max	0.868	0.530

^arms thermal-vibration amplitude 0.0759 Å.

^bF. H. Eisen, unpublished data.

potential with thermal effects included clearly gives the best result for the random stopping power, the agreement is not nearly as good as was achieved for gold. While this may be attributable to experimental uncertainties, it is more likely to originate in limitations of the potentials used. The strongly covalent nature of solid Si makes it certain that the Hartree potential used here is rather approximate. Nevertheless, the Si experiments fit the model in a convincing manner.

CONCLUSION

The substantial success of the model described above in accounting for both planar-channeling data and random stopping powers in terms of theoretically well-founded potential functions strongly supports its essential correctness and lends credence to predictions made from the model. In addition to the geometrical effects on the energy-loss spectra which have been discussed before,^{1,2,4,5} the model predicts a dependence of the observed spectra on the target temperature, beyond that due to thermal changes in volume. The potential factor in Eq. (17) will decrease with increasing temperature because of the temperature dependence of the thermal vibrations. The only available experiments,²¹ however, show that the random stopping powers of metals are essentially independent of temperature, in agreement with theoretical considerations.²² On the somewhat speculative assumption that the minimum stopping power s_0 is independent of temperature, the model implies that s_1 must vary with temperature in a manner compensating for thermal changes in the potential. Using the Debye theory to estimate the thermal change in the vibration amplitudes²³ of gold, it is found that s_1 should decrease by about 15% between room temperature and liquid-nitrogen temperature and by another 5% at 0°K. This change should produce easily measurable effects on the energy-loss spectra: As the temperature is lowered, the parameter β will decrease, leading to a decreased separation between peaks in the spectra (compare the experimental spectra in Refs. 2-6). In fact, an interesting test of the model can be constructed by measuring spectra for various pathlengths at two (or more) temperatures. Plots of the stopping power of channeled ions as a function of their oscillation frequencies should then extrapolate to a crossing at the value of s_0 , providing an independent means of locating the center of the channel. From the temperature dependence of the slopes of these plots information could be obtained about the interaction potential and about thermal-vibration amplitudes as well.

It has been suggested^{2,11} that the stopping power of channeled ions should be proportional to the local electron density in the target and that this in turn should be related to the potential $V_2(x)$ through

Poisson's equation. While there seem to be no very compelling reasons for either of these suggestions to be correct, it is nevertheless instructive to consider the circumstances under which they would lead to a proportionality between the stopping power and oscillation frequency of channeled ions. Defining

$$f(x) = \{2[V_2(x) - V_2(0)]/V_2''(0)\}^{1/2}, \quad (20)$$

the model stopping power may be written as

$$S(x, E) = s_0 - s_1 + s_1 f'(x), \quad (21)$$

where the prime represents differentiation with respect to x . Similarly, using Poisson's equation to relate the local electron density to the planar-channel potential, the stopping power should be

$$S(x, E) = \gamma + (s_0 - \gamma)\{f(x)f''(x) + [f'(x)]^2\}, \quad (22)$$

where γ is a constant. These two representations of the stopping power may be equated to give a differential equation which is to be solved subject to the boundary conditions $f(0) = 0$ and $f'(0) = 1$. The only solution which meets both of these conditions is $f(x) = x$; that is, the two representations of the stopping power are the same only for the harmonic potential

$$V_2(x) = V_2(0) + \frac{1}{2} V_2''(0)x^2, \quad (23)$$

for which the stopping power has everywhere the value s_0 . This result is trivial since not only is the stopping power independent of the oscillation amplitude, but so also is the oscillation frequency: Just those features of the model which are required to account for the experimental observations have disappeared. Of course, it should not really be surprising that this is so. The interaction potential is concerned with the spatial distribution of all of the electrons in the system, whatever their quantum states, since this is what controls the screening of the nuclear charges. In contrast, the stopping power is determined by those electrons which can be excited to higher states and should involve not only their density but also the probability of excitation. It must be said, then, that the origin of Eq. (4)—the proportionality of stopping power to channel oscillation frequency—is not understood. The fact that it seems to apply equally well at rather low velocities (I ions in Au), near the maximum of the (random) stopping-power curve (O ions in Au), and in the region of applicability of the Bethe-Bloch equation (He ions in Au, H ions in Si) requires that the proportionality be insensitive to the details of stopping-power theory. This might imply its origin in some aspect of the dynamical problem instead.

ACKNOWLEDGMENTS

It is a pleasure to express my sincere appreciation to B. R. Appleton, S. Datz, F. H. Eisen, and C. D. Moak for many stimulating conversations and for providing the experimental data used herein.

I am also grateful to W. E. Atkinson, J. H. Barrett, D. K. Holmes, and T. S. Noggle for useful discussions and helpful criticisms in the course of this work, and to C. W. Nestor, Jr., for guidance in using the machine program for the relativistic Hartree calculations.

*Research sponsored by the U. S. Atomic Energy Commission under contract with Union Carbide Corporation.

¹M. T. Robinson, Phys. Rev. 179, 327 (1969).

²H. O. Lutz, S. Datz, C. D. Moak, and T. S. Noggle, Phys. Rev. Letters 17, 285 (1966).

³W. M. Gibson, J. B. Rasmussen, P. Ambrosius-Olesen, and C. J. Andreen, Can. J. Phys. 46, 551 (1968).

⁴S. Datz, C. D. Moak, T. S. Noggle, B. R. Appleton, and H. O. Lutz, Phys. Rev. 179, 315 (1969).

⁵S. Datz, C. D. Moak, B. R. Appleton, M. T. Robinson, and O. S. Oen, in *Atomic Collision Phenomena in Solids*, edited by D. W. Palmer, M. W. Thompson, and P. D. Townsend (North-Holland, Amsterdam, 1970), p. 374.

⁶B. R. Appleton, S. Datz, C. D. Moak, and M. T. Robinson, first preceding paper, Phys. Rev. B 4, 1452 (1971).

⁷F. H. Eisen and M. T. Robinson, second preceding paper, Phys. Rev. B 4, 1457 (1971).

⁸See, for example, O. Klein, Z. Physik 76, 226 (1932).

⁹J. Lindhard, Kgl. Danske Videnskab. Selskab, Mat.-Fys. Medd. 34, No. 14 (1965).

¹⁰See, for example, M. T. Robinson, in *Atomic Collision Phenomena in Solids*, edited by D. W. Palmer,

M. W. Thompson, and P. D. Townsend (North-Holland, Amsterdam, 1970), p. 66.

¹¹E. S. Machlin, S. Petralia, A. Desalvo, R. Rosa, and F. Zignani, Phil. Mag. 22, 101 (1970).

¹²M. W. Thompson, Phil. Mag. 18, 377 (1968).

¹³A. A. Abrahamson, Phys. Rev. 178, 76 (1969).

¹⁴P. Gombas, in *Handbuch der Physik*, edited by S. Flügge (Springer, Berlin, 1956), Vol. 36, p. 109.

¹⁵G. Molière, Z. Naturforsch. 2a, 133 (1947).

¹⁶T. C. Tucker, L. D. Roberts, C. W. Nestor, Jr., and T. A. Carlson, Phys. Rev. 178, 998 (1969).

¹⁷C. Erginsoy, in *Interaction of Radiation with Solids*, edited by A. Bishay (Plenum, New York, 1967), p. 341; Phys. Rev. Letters 15, 360 (1965).

¹⁸There is an error in Eq. (16) of Ref. 1. The second and third terms of the sum should contain additional factors e^{-3bt} and e^{-19bt} , respectively.

¹⁹V. Synacek, H. Chessin, and M. Simerska, Acta Cryst. A26, 108 (1970).

²⁰B. W. Batterman and D. R. Chipman, Phys. Rev. 127, 690 (1962).

²¹A. N. Gerritsen, Physica 12, 311 (1946).

²²H. A. Kramers, Physica 13, 401 (1946).

²³M. Blackman, in *Handbuch der Physik*, edited by S. Flügge (Springer, Berlin, 1955), Vol. 36, p. 377.